

## Shortcomings of the $R$ -matrix method for treating dielectronic recombination

T. W. Gorczyca

*Department of Physics, Western Michigan University, Kalamazoo, Michigan 49008*

N. R. Badnell

*Department of Physics and Applied Physics, University of Strathclyde, Glasgow, G4 0NG, United Kingdom*

D. W. Savin

*Columbia Astrophysics Laboratory, Columbia University, New York, New York 10027*

(Received 11 October 2001; published 6 June 2002)

By performing radiation-damped  $R$ -matrix scattering calculations for the photorecombination of  $\text{Fe}^{17+}$  forming  $\text{Fe}^{16+}$ , we demonstrate and discuss the difficulties and fundamental inaccuracies associated with the  $R$ -matrix method for treating dielectronic recombination (DR). Our  $R$ -matrix results significantly improve upon earlier  $R$ -matrix results for this ion. However, we show theoretically that all  $R$ -matrix methods are unable to account accurately for the phenomenon of radiative decay followed by autoionization. For  $\text{Fe}^{17+}$ , we demonstrate numerically that this results in an overestimate of the DR cross section at the series limit, which tends to our analytically predicted amount of 40%. We further comment on the need for fine resonance resolution and the inclusion of radiation damping effects. Overall, slightly better agreement with experiment is still found with the results of perturbative calculations, which are computationally more efficient than  $R$ -matrix calculations by more than two orders of magnitude.

DOI: 10.1103/PhysRevA.65.062707

PACS number(s): 34.80.Lx, 32.80.Fb, 34.80.Kw, 32.80.Dz

### I. INTRODUCTION

The need for reliable dielectronic recombination (DR) rate coefficients has increased dramatically with the recent launches of the new high-resolution x-ray satellites *Chandra* and *XMM-Newton*. Observations by these satellites of active galactic nuclei, quasars, and x-ray binaries have resulted in high resolution spectra that are rich in absorption and emission lines [1–5] and which require reliable atomic data to interpret. Of particular importance are the DR rate coefficients for iron  $L$ -shell ions at the low temperatures relevant to the above cosmic sources. These DR rate coefficients are important for understanding the ionization structure, line emission, and thermal structure of these plasmas [6–8].

To address the need for reliable low-temperature iron  $L$ -shell DR rate coefficients, we are carrying out a series of combined experimental and theoretical studies [6,9,10]. Measurements are being carried out using the heavy-ion test storage ring at the Max Planck Institute for Nuclear Physics in Heidelberg, Germany. Calculations, to date, have been performed using the perturbative multiconfiguration Breit-Pauli code AUTOSTRUCTURE [11] and a multiconfiguration Dirac-Fock (MCDHF) code [12] for  $\text{Fe}^{17+}$ ,  $\text{Fe}^{18+}$ , and  $\text{Fe}^{19+}$  [6,9,10]. For  $\text{Fe}^{19+}$  [10], calculations were also carried out using the HULLAC suite of codes [13] and a radiation-damped  $R$ -matrix method [14], and a detailed comparison made between all four theoretical results and the experimental ones was made.

Recently, the  $R$ -matrix method was used by another group to calculate electron-ion recombination data for  $\text{Fe}^{17+}$  [15,16]. For DR resonances of the  $2s^2 2p^5 ({}^2P_{1/2})nl$  series (see Fig. 1 of Ref. [15] and Fig. 6 of Ref. [16]), these results are in poorer agreement with experiment than are the earlier perturbative results. These resonances are important as they

make a significant contribution to the total recombination rate coefficient at temperatures where  $\text{Fe}^{17+}$  is predicted to peak in abundance in an optically thin, low-density, and photoionized gas with cosmic abundances [6,8]. Also, compared to experimental and perturbative results, these earlier  $R$ -matrix results [15,16] overestimated the higher- $n$  DR resonances of the  $2s2p^6nl$  series by  $\approx 40\%$  at the series limit. These two points would seem to suggest that the  $R$ -matrix method is not particularly well suited for determining reliable DR rate coefficients.

Here we reexamine DR of  $\text{Fe}^{17+}$  using a radiation-damped  $R$ -matrix method. We outline our present theoretical methodology in Sec. II. We present our results in Sec. III, and compare with earlier experimental, perturbative, and  $R$ -matrix results. Difficulties with resonance resolution, radiative decay to autoionizing states, and damping of resonances are also discussed. In Sec. IV, we address the utility of frame transformation techniques, focusing on the inverse process photoionization of  $\text{Fe}^{16+}$ . Concluding remarks are given in Sec. V.

### II. THEORETICAL METHODOLOGY

We rely on the  $R$ -matrix method [17], using the Rmax [18] suite of codes [19], which include Breit-Pauli [20] and radiation-damping [14] effects. We point out briefly how the various radiative effects are included by considering the pathways of interest listed below.

Electrons can recombine with  $\text{Fe}^{17+}$  in the  $2s^2 2p^5 ({}^2P_{3/2})$  ground state (which we denote as  $2p_{3/2}^{-1}$ ) via

$$e^- + 2p_{3/2}^{-1} \rightarrow 2p_{3/2}^{-1}nl + h\nu \quad (n \geq 2), \quad (1)$$

$$\begin{aligned} e^- + 2p_{3/2}^{-1} &\leftrightarrow 2p_{1/2}^{-1}nl \quad (n \geq 18) \\ &\rightarrow 2p_{1/2}^{-1}n'l' + h\nu \quad (n' < 18), \end{aligned} \quad (2)$$

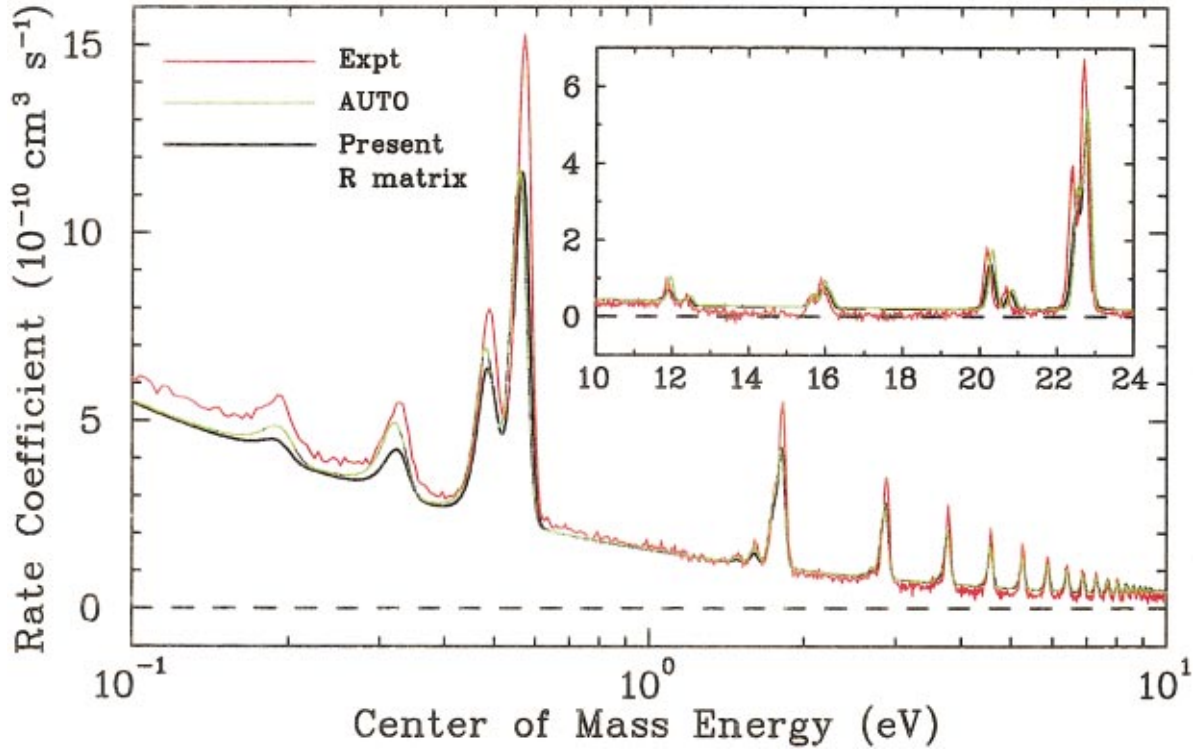
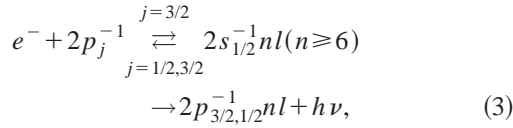
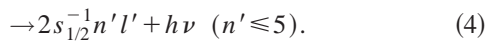


FIG. 1. (Color)  $\text{Fe}^{17+}$  to  $\text{Fe}^{16+}$  electron-ion recombination for collision energies from 0.1–24 eV. The *black curve* shows our *R*-matrix results that have been multiplied by the relative electron-ion velocity and convolved with the energy spread of Refs. [6,9]. The experimental (Expt.) results [6,9] and perturbative AUTOSTRUCTURE (AUTO) results [6] are given by the *red curve* and the *green curve*, respectively. The  $2s^2 2p^5(^2P_{1/2})nl$  DR resonances can be clearly seen below the series limit of  $\approx 13$  eV. The resonances between  $\approx 12$ –24 eV are the  $n=6$  members of the  $2s 2p^6(^2S_{1/2})nl$  DR series. Differences between the experimental and theoretical nonresonant RR background is believed to be an artifact due to the subtraction of charge transfer signal from the measured recombination results.



or



The nonresonant radiative recombination (RR) in Eq. (1), and the resonant valence electron decay in Eqs. (2) and (4), are included by using an inner-region optical potential for  $2 \leq n \leq 3$  and an outer-region imaginary hydrogenic correction to the scattering matrices for  $n \geq 4$ . The earlier *R*-matrix work [15,16] relied on an inverse photoionization approach, using the Milne relation to convert photoionization cross sections to RR+DR cross sections. However, they did not account for the valence radiative decay in Eq. (2) to states with  $11 \leq n' < 18$ . Furthermore, they did not include radiative-damping effects, which will be discussed in Sec. III C.

The core radiative decay in Eq. (3) is included in our present approach by adding an imaginary term to the effective quantum number, as originated by Hickman [21]. This method has been shown [22] to be more rigorous than that of Bell and Seaton [23], which was used earlier [15,16] for  $n > 10$ , but the two methods are expected to give nearly iden-

tical results. Further details of our radiation-damped *R*-matrix method are published elsewhere [10,24,25].

Our *R*-matrix calculations were carried out up to  $J=25$ . At low energies, we topped up the nonresonant (i.e., RR) portion of these results using AUTOSTRUCTURE calculations for  $J$  up to 125. This was done for both our RR+DR and RR-only *R*-matrix results. *R*-matrix RR calculations [for Eq. (1)] were carried out by eliminating all closed channels, i.e., by performing a one-state calculation including only the  $2s^2 2p^5(^2P_{3/2})$  state—this eliminates all resonances by definition.

For the atomic structure, we first performed a Hartree-Fock calculation [26] for the  $1s^2 2s^2 2p^5$  ground state of  $\text{Fe}^{17+}$ . These orbitals were then used to describe the  $1s^2 2s^2 2p^5(^2P_{3/2})$ ,  $1s^2 2s^2 2p^5(^2P_{1/2})$ , and  $1s^2 2s 2p^6(^2S_{1/2})$  target states. A continuum/bound basis consisting of 20 orbitals per angular momentum was then used to describe the scattering/resonance states.

Lastly, we use the extremely efficient multichannel quantum defect theory (MQDT) [27,28]. The unphysical scattering and dipole matrices (in the MQDT formulation), which have little energy dependence, are computed on a coarse energy mesh. These are then interpolated for the tens of millions of energy points actually needed to resolve narrow resonance structure before applying the MQDT reduction to physical quantities. Thus, the actual *R*-matrix calculations

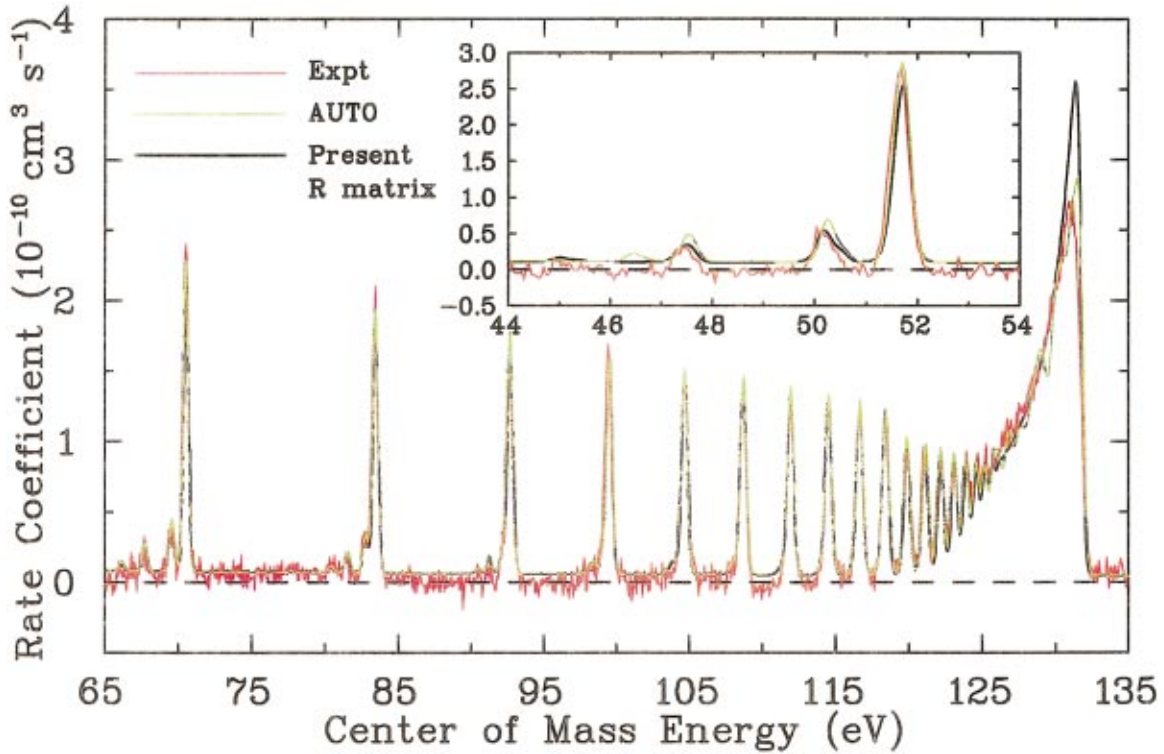


FIG. 2. (Color) Same as Fig. 1. The  $n=7$  members (inset) and higher lying members of the  $2s^2 2p^6(^2S_{1/2})nl$  DR series can be clearly seen converging to the series limit at  $\approx 132$  eV.

are performed for a few hundred energies, and algebraic equations are applied elsewhere, resulting in a computational savings of large orders of magnitude.

### III. $\text{Fe}^{17+}$ PHOTORECOMBINATION RESULTS

In this section, we first compare our present *R*-matrix results to the earlier experimental and perturbative results [6,9], focusing separately on the  $2p \rightarrow 2p$  and  $2s \rightarrow 2p$  core excitations. Second, the effect of radiation damping is quantified. Third, we compare our *R*-matrix and perturbative results to those from earlier *R*-matrix calculations presented in Refs. [15,16]. In Figs. 1 and 2, we present our *R*-matrix results for the photorecombination (RR+DR) of  $\text{Fe}^{17+}$ , along with the experimental and perturbative AUTOSTRUCTURE results of Refs. [6,9].

#### A. The $2s^2 2p^5(^2P_{1/2})nl$ series: Resonance resolution

In the region between 0–13 eV shown in Fig. 1, we see the  $2s^2 2p^5(^2P_{1/2})nl$  DR series, which autoionizes or radiatively decays via the pathways shown in Eq. (2). Since both decays involve the valence electron, the resonances have autoionization and radiative widths that scale as  $n^{-3}$ —typical total widths are of the order  $0.1n^{-3}$  eV. Hence, an extremely fine energy mesh is required to delineate this series. We used  $10^7$  energy points for the region between 0–13 eV (i.e., a linear mesh with a step size of  $1.3 \times 10^{-6}$  eV) in order to obtain the results shown. Our *R*-matrix results clearly reproduce the measured structure of the  $2s^2 2p^5(^2P_{1/2})nl$  series shown in Fig. 1. However, the

integrated theoretical resonance strengths lie below experiment, by  $\approx 25$ –30% for the lowest resonance complexes. This discrepancy increases to  $\approx 50\%$  at the series limit. Note that our *R*-matrix results above 0.5 eV are virtually indistinguishable from the AUTOSTRUCTURE results on the scale of Fig. 1, which confirms that we have resolved all significant resonance contributions.

The earlier *R*-matrix calculation [15] used a mesh size of  $\geq 1.0 \times 10^{-4}$  eV to span 0–13 eV, a hundred or more times coarser than our mesh. As can be seen in Fig. 1 of Ref. [15], their results were unable even qualitatively to reproduce the experimental results [6,9] for the  $2s^2 2p^5(^2P_{1/2})nl$  series. This is most likely due to their failure to resolve narrow resonances. The subsequent calculations of Ref. [16] used a finer grid for studying selected resonances, but as can be seen in Fig. 6 of that work, there is no improvement for the  $2s^2 2p^5(^2P_{1/2})nl$  series.

There are two other shortcomings in the calculations of Refs. [15,16] which are worth noting. First, the calculations did not include DR to states for  $11 \leq n' < 18$  [see Eq. (2)]. We determine this to result in an  $\approx 15\%$  underestimate of the DR resonance strengths. Second, the calculations did not include radiation damping, which we find has an approximately 50% reduction effect on the integrated resonance strengths, as discussed in Sec. III C.

Resolution is one of the main difficulties of using the *R*-matrix method to calculate DR rate coefficients. Unlike the case of electron-impact excitation, narrow (but high) resonances are just as important a contribution to the DR rate coefficient as broader (but lower) resonances since the



(energy-averaged) DR resonance strength depends on the (small) radiative width, but is independent of the (larger) autoionization width [29,30]. Gailitis-type averaging techniques, even when applicable [e.g., for the  $2s2p^6(^2S_{1/2})$  series], solve the resolution problem. But in general, this method is always limited to energy regions free from interloper resonances attached to higher thresholds (which must still be resolved). Also, averaging cannot be used for noncore stabilizing series, such as the  $2s^22p^5(^2P_{1/2})nl$  one in the present study. Perturbative methods, on the other hand, do not suffer from the problem of resonance resolution since all resonance positions and widths are computed directly and analytically convoluted for complete resolution. For just the  $2s^22p^5(^2P_{1/2})nl$  series, however, inverse photoionization techniques *could* be applied by analytically preconvolving the resonances *as long as an MQDT* formulation is used [30,31], since photoionization in this region has only one open channel.

### B. The $2s2p^6(^2S_{1/2})nl$ series: Radiative decay to autoionizing states

For the region from  $\approx 13$  eV to the  $2s2p^6(^2S_{1/2})nl$  series limit at  $\approx 132$  eV, the autoionization widths of these resonances scale as  $n^{-3}$ , while the core radiative width for each of these resonances is independent of  $n$ . Delineating the entire series thus requires an energy mesh size only somewhat smaller than this constant radiative width, given by  $\Gamma_{2s2p^6 \rightarrow 2s^22p^5}^r = 7.6 \times 10^{-5}$  eV. We use  $10^7$  energy points over this region, for a mesh size of  $1.3 \times 10^{-5}$  eV or, rather, roughly six points per radiative width.

As mentioned above, the analytic (Gailitis-type) averaging including damping, as was done for  $n > 10$  in the earlier  $R$ -matrix work [15,16], can be safely used for this series, since it is free from interloper resonances attached to higher thresholds, and would allow a much coarser mesh to be used. However, averaging washes out the resonance structure and we wish to make a precise comparison with experiment. Here, we use a suitably fine mesh so as to resolve this series unambiguously. We also omit contributions from resonances with principal quantum number  $n > 124$  in order to compare with experiment, which does not detect these resonances due to field ionization. The contribution from  $n > 124$  increases the theoretical results at the series limit by  $\approx 10\%$ , but ignoring this contribution has a  $\lesssim 2\%$  effect on the Maxwellian DR rate coefficient [9].

Figures 1 and 2 show that our  $R$ -matrix and AUTOSTRUC-TURE results underestimate the strength of the  $2s2p^6(^2S_{1/2})6l$  and, to a lesser extent,  $7l$  resonances. Agreement between our  $R$ -matrix theoretical results and experimental results is better for the higher-lying  $2s2p^6(^2S_{1/2})nl$  resonances, until just below the series limit at  $\approx 132$  eV. About 13 eV below this limit, radiative “stabilization” to the  $2s^22p^5(^2P_{1/2})nl$  states is preferentially followed by autoionization of these states (for  $n \geq 18$ ) to the  $2s^22p^5(^2P_{3/2}) + e^-$  continuum. This “stabilization” ultimately makes only a small contribution to DR forming stable bound  $\text{Fe}^{16+}$  states—note the resulting drop above  $\approx 120$  eV in Fig. 2. In our  $R$ -matrix calculations, we therefore neglect this width in

the optical potential. However, this radiative width is a significant contribution to the total width as,  $n \rightarrow \infty$ , and neglecting it eventually leads to an overestimate of DR at the series limit.

It helps to consider this multistep process from a perturbative point of view, for which the energy-averaged DR rate coefficient can be expressed as

$$\langle \nu \sigma_{DR} \rangle \propto \Gamma_{3/2}^a \left( \frac{\Gamma_{val}^r + \Gamma_{core,3/2}^r}{\sum_j \Gamma_j^a + \Gamma_{val}^r + \sum_j \Gamma_{core,j}^r} \right) \quad (5)$$

$$\xrightarrow{n \rightarrow \infty} \Gamma_{3/2}^a \left( \frac{\Gamma_{core,3/2}^r}{\sum_j \Gamma_{core,j}^r} \right) \quad (6)$$

$$= \Gamma_{3/2}^a \left( \frac{5}{7} \right). \quad (7)$$

Here  $j = 1/2$  and  $3/2$ ,  $\Gamma_j^a$  is the autoionization width to the  $2s^22p^5(^2P_j) \epsilon l$  continuum, and  $\Gamma_{val}^r$  is the sum of valence radiative widths occurring in Eq. (4) [all of the above widths go to zero as  $n \rightarrow \infty$ ].  $\Gamma_{core,3/2}^r = 2.0 \times 10^{-6}$  a.u. (atomic units) and  $\Gamma_{core,1/2}^r = 0.8 \times 10^{-6}$  a.u. are the core radiative widths in Eq. (3).

In radiation-damped  $R$ -matrix methods—both Bell and Seaton, as used earlier [15,16], and Hickman and Robicheaux, as used here—only a *single* radiative loss term is present in the formulation and it is used to represent both the radiative width contributing to the DR *and* the total radiative width of the resonance. When the two differ, we are forced to make a choice. Using the total radiative width would give no drop in the rate coefficient above 120 eV, a drop which the experiment clearly shows, so we use the radiative width to nonautoionizing states only. In fact, it doesn’t matter which radiative width we choose in the series limit because they both result in the same overestimate since, in the perturbative picture [Eqs. (5) and (6)], the same radiative width appears in the numerator and denominator, i.e., the  $R$ -matrix method introduces no  $5/7$  factor, as in Eq. (7). Therefore, the resonances are overestimated by a factor of  $7/5$ , or are 40% too high, at the series limit.

Equation (7), without the  $5/7$  factor, is just a restatement of the continuity of the (averaged) DR cross section across threshold, joining onto the electron-impact excitation cross section. While an important check on  $\Gamma^a$ , it says nothing about the validity of the radiative widths being used. The  $5/7$  factor does not mean that perturbation theory violates unitarity, since the electron and photon flux are still conserved, but not all of the photon flux counts as stable recombination, only  $5/7$  of it. The remaining  $2/7$  of the photon flux subsequently leads to electron emission again.

Figure 2 shows that our  $R$ -matrix series limit results peak at  $\approx 3.6 \times 10^{-10} \text{ cm}^3 \text{ s}^{-1}$ . The earlier  $R$ -matrix study [15,16] found  $3.87 \times 10^{-10} \text{ cm}^3 \text{ s}^{-1}$ . The experimental value of Refs. [6,9] shown in Fig. 2 peaks at  $\approx 2.7 \times 10^{-10} \text{ cm}^3 \text{ s}^{-1}$ . Our  $R$  matrix results overestimate experiment by  $\approx 30\%$  at the series limit. As the convolution resolution is increased, this overestimate tends towards the theoretical limit of 40%.

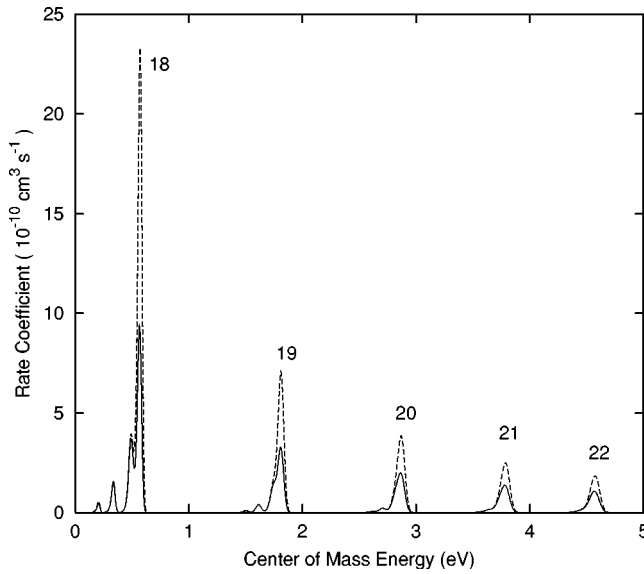


FIG. 3. Comparison of undamped (*dashed curve*) and damped (*solid curve*) DR rate coefficients for the  $2p^5(^2P_{1/2})nl$   $n=18-22$  series. The resonances have been convolved with the experimental resolution of Refs. [6,9].

### C. Radiation damping of resonances

When the radiative width becomes comparable to, or greater than, the autoionization width, the resonances become “damped.” In other words, the computed resonance strength is reduced compared to results from a calculation that ignores the broadening due to the radiative width.

In Fig. 3, we compare AUTOSTRUCTURE results for the  $2s^22p^5(^2P_{1/2})nl$  series for  $n=18-22$ , both with and without damping. It is clearly seen that for this lower series, the undamped resonance strengths are much greater than the damped ones. Since both the radiative and autoionization widths scale as  $n^{-3}$ , this damping ratio remains fairly constant as  $n \rightarrow \infty$ ; we find that the damped  $n=22$  resonances are reduced by a factor of  $\approx 0.62$ , or that neglecting radiation damping gives an integrated resonance strength 60% too large. Thus, calculations that ignore radiation damping effects *should* grossly overestimate the DR rate coefficients, provided that the resonances are fully resolved in the first place. Conversely, calculations that do not fully resolve the resonances will tend to underestimate the DR rate coefficients. The inverse photoionization method used in the earlier *R* matrix study [15,16] did not include radiation damping in their final results. The fact that the reported resonance strengths for  $n=18-20$  of Ref. [16] appear to be in excellent agreement with the measured values is most probably due to inadequate resolution being used, fortuitously canceling the effect due to their neglect of radiation damping for this series. In the absence of experimental data or damped theoretical results, large uncertainties exist in undamped *R*-matrix results since the contribution from resonances that should be damped is not known.

Damped and undamped results for the  $2s2p^6(^2S_{1/2})nl$  series for  $n=7-10$  are shown in Fig. 4, and the effect of damping here, while less than for the  $2s^22p^5(^2P_{1/2})nl$  resonances, is not negligible, increasing to an  $\approx 2/3$  reduction

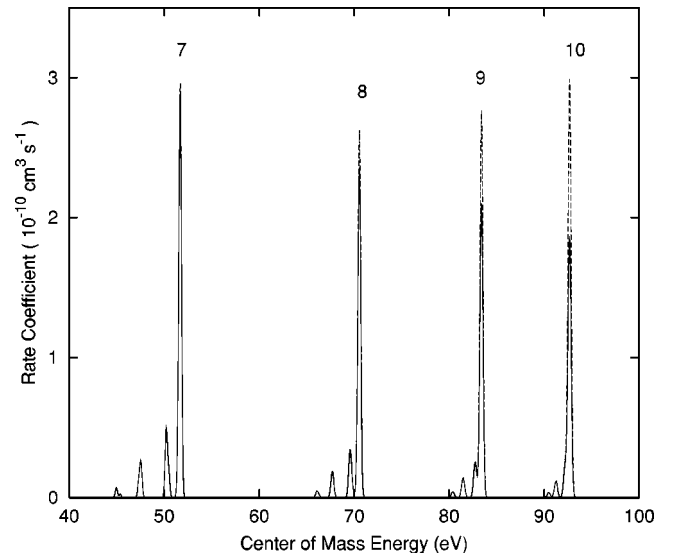


FIG. 4. Comparison of undamped (*dashed curve*) and damped (*solid curve*) DR rate coefficients for the  $2s2p^6(^2S_{1/2})nl$   $n=7-10$  series. The resonances have been convolved with the experimental energy resolution of Refs. [6,9].

factor for  $n=10$ , i.e., the undamped resonance strengths are  $\approx 50\%$  too large here. As  $n$  increases, the radiative width, which is independent of  $n$ , eventually dominates the autoionization width, which scales as  $n^{-3}$ , so damping becomes crucial as  $n \rightarrow \infty$ . Of course, in our present *R*-matrix method, using the Hickman and Robicheaux formalism, or the earlier *R*-matrix method, which uses the Bell and Seaton formalism for  $n > 10$ , damping effects are included. However, the earlier *R*-matrix calculations [15,16] did not include damping for the  $n=7-10$  members of the  $2s2p^6(^2S_{1/2})nl$  series.

### D. Comparison to earlier results

In Fig. 5, we present our *R*-matrix RR+DR Maxwellian rate coefficient results. We also show the experimental and perturbative DR results [6,9], to which we have added our topped-up *R*-matrix RR results. In the predicted formation zone for  $\text{Fe}^{17+}$  in an optically-thin, low-density, photoionized gas with cosmic abundances [8], our *R*-matrix results are in excellent agreement with the AUTOSTRUCTURE and MCFD results. The results of all three calculations lie  $\approx 10\%$  below the experimental rate coefficient [6,9]. The earlier *R*-matrix results [15,16] are also shown and are in poorer agreement with experiment—they lie  $\approx 20\%$  below it. This difference in the total recombination rate coefficient implies a much larger discrepancy in the DR portion of the earlier results. For reference, we show our topped-up *R*-matrix RR results, which are in good agreement with the results of Arnaud and Raymond [32] over the temperature range shown.

To summarize, there are significant differences between the experimental results and all theoretical results, both past and present. The question is, why do these discrepancies exist? It is important to include as many physical processes as is computationally possible in the theoretical calculations in order to assess the current status of photorecombination re-

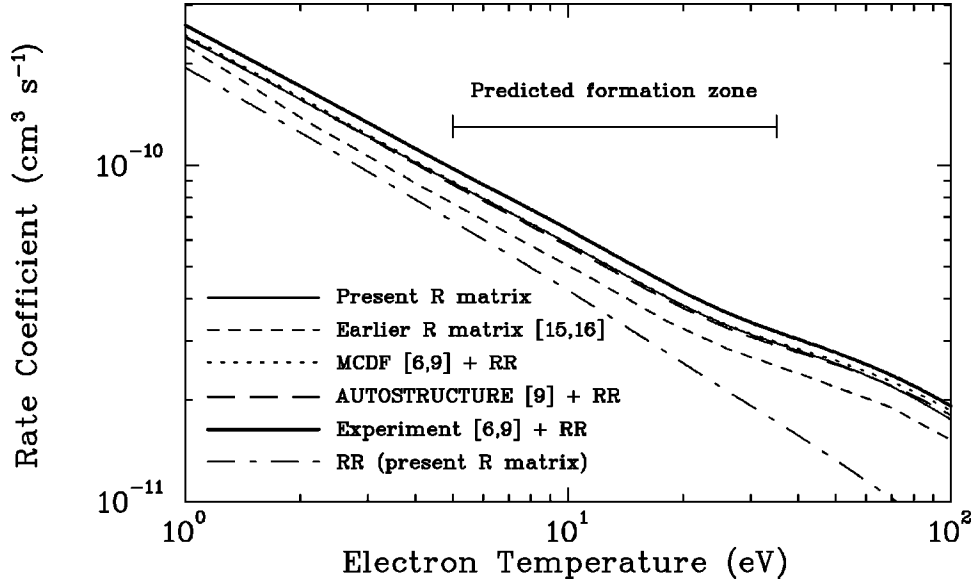


FIG. 5. Maxwellian rate coefficient for photorecombination (RR+DR) of  $\text{Fe}^{17+}$  to  $\text{Fe}^{16+}$ . The *thin solid curve* shows our  $R$ -matrix results and the *short dashed curve* those of Refs. [15,16]. The published experimental (*thick solid curve*, [6,9]), perturbative MCDF (*dotted curve*, [6,9]), and AUTOSTRUCTURE (*long dashed curve*, [6]) DR results are also shown. We have added our topped-up,  $R$ -matrix RR rate coefficient (*dotted-long-dashed curve*) to the experimental and perturbative DR rate coefficients.

results, in particular, to assess the accuracy of theoretical versus experimental results.

In the present study, we have identified several effects that may be important: (1) inclusion of radiative decay channels for  $n=11-17$  in Eq. (1), which we find to account for  $\approx 10-15\%$  of the  $2p \rightarrow 2p$  resonance strengths; (2) complete resolution of the  $2s^2 2p^5 ({}^2P_{1/2})nl$  resonance series using tens of millions of energy points, which includes narrow but strong resonances that would be missed with a coarser mesh; (3) radiation damping, which reduces the  $2p^5 ({}^2P_{1/2})nl$  resonance strengths by  $\approx 60\%$ ; (4) autoionization of radiatively “stabilized” states, which here reduces the  $2s 2p^6 ({}^2S_{1/2})nl$  series limit by a factor of  $5/7$ ; and (5) interference effects, which we assess to be negligible by the excellent agreement between perturbative AUTOSTRUCTURE and present  $R$ -matrix results. The earlier  $R$ -matrix calculations [15,16] did *not* include the first four of these effects, and consequently obtained results with a mixture of underestimates and overestimates, giving an unreliable rate coefficient. Our present  $R$ -matrix calculations did not include (4) and therefore overestimated the  $2s 2p^6 ({}^2S_{1/2})nl$  series limit by  $\approx 7/5$  at 132 eV. The present perturbative calculations did not include (5), which we find to be unimportant, but give better results than the  $R$ -matrix method since effect (4) is easily included.

#### IV. PHOTOIONIZATION OF $\text{Fe}^{16+}$

The inverse process of photorecombination of  $\text{Fe}^{17+}$ , where an incoming electron is captured and a photon is released, is photoionization of  $\text{Fe}^{16+}$ , where an incident photon is absorbed and an electron is emitted [the reverse of Eq. (1) for  $n=2$ ]. For complex cases where a large degree of electron correlation is necessary, an extremely efficient approach for also including relativistic effects is the frame transformation method [28,33]. In the case of doubly excited (i.e.,

highly correlated), spin-forbidden (i.e., requiring relativistic effects) resonances in Ne, it was found that a frame transformation calculation [34] reproduced complex spectra observed from synchrotron measurements to a remarkable degree [35]. The complexity of the correlation required to describe these states made full Breit-Pauli  $R$ -matrix calculations impossible with the available computers.

Frame transformation methods are extremely useful for simultaneously including complex correlation and relativistic effects, and yield theoretical results that are essentially identical to more elaborate Breit-Pauli ones. For instance, comparisons between the two methods for the simpler cases of photoionization of  $\text{Fe}^{16+}$  [36] and  $\text{Fe}^{14+}$  [37], and for the more complex case of electron impact excitation of  $\text{Ni}^{4+}$  [38], showed excellent agreement. The main approximation in the frame transformation method is that the lowest lying resonances do not have fine structure effects incorporated in their description, but this does not significantly affect the computed convoluted cross sections [28,37,38].

In this light, we wish to correct an unsubstantiated claim by Ref. [16] concerning photoionization of  $\text{Fe}^{16+}$ . There it is stated, in reference to earlier frame transformation methods for  $\text{Fe}^{16+}$  [36] that “photoionization of other highly charged ions may not be amenable to the approximations described in [36].” They give no justification for this statement. Instead, they ignore the fact that it is *precisely* for more complex systems that *only* the frame transformation method is able to compute reliable photoionization data with the available computational resources. In our present study, we were able to use the minimal configuration description for all the processes listed in Eqs. (1)–(4), and the bulk of the computational effort went into repeating the MQDT equations at tens of millions of energy points, which must be done using either Breit-Pauli or frame transformation methods. Therefore, we

simply relied on the Breit-Pauli method; for more complex cases of low-charged, open-shell Fe ions, this will not be true, and frame transformation methods are more practical.

## V. CONCLUSION

We have performed *R*-matrix calculations for photorecombination (RR+DR) of Fe<sup>17+</sup> and are able to obtain results that are in reasonable agreement with experiment, provided that one uses  $\geq 100$  times more energy points for the  $2s^2 2p^5 ({}^2P_{1/2})nl$  series than were used in an earlier *R*-matrix calculation [15]. Radiative damping and decay to all final accessible states must also be included. However, we have discovered a fundamental flaw of all current radiation-damped *R*-matrix methods: they do not accurately take into account the process of radiative decay followed by autoionization, and therefore overestimate DR at the series limit. In the case of the Fe<sup>17+</sup>  $2s 2p^6 ({}^2S_{1/2})nl$  series, we observe the overestimate tending to the analytically predicted amount of 40%. This overestimate was seen in, but not explained by, the earlier *R*-matrix studies [15,16].

Our work finds that perturbative methods are computationally more efficient (by a factor of 300 in the case of AUTOSTRUCTURE), and give results [6] which turn out to reproduce the experimental results somewhat better than do those of the *R*-matrix method, even when the *R*-matrix calculation fully resolves all contributing resonances and includes radiation damping. We note that AUTOSTRUCTURE consistently computes all contributing partial and total rate coefficients for RR and DR (via both  $\Delta n = 0$  and  $\Delta n > 0$  core excitations). Furthermore, the separation of DR into  $\Delta n = 0$  and  $\Delta n > 0$  contributions is a convenience, not a requirement of the approach.

Given infinite computing power, the *R*-matrix method does give a more complete description of the scattering process than do lowest order perturbative methods in that direct-

resonant interference is included. However, as is discussed at length by Pindzola *et al.* [39], interference is insignificant for the determination of accurate DR cross sections of multiply charged systems. Indeed, we have always found very good agreement between radiation-damped *R*-matrix results and those from AUTOSTRUCTURE for the DR of many ionic systems [10,25,30,40]. Here we also find the natural physical separation of RR and DR into independent processes to be a highly accurate approximation (the quantum mechanical interference effect is very small) as is the neglect of interacting resonances—note the nearly identical theoretical results in Figs. 1 and 2. Both approximations have no significant effect on plasma modeling—see Pindzola *et al.* [39] for a detailed analysis of these effects—while the use of distorted waves is known to be accurate for atoms at least a few times ionized.

Comparison between perturbative and *R*-matrix results does provide a consistency check on various aspects of the calculations, and helps to reveal the more important underlying physical effects. However, our present study demonstrates that the *R*-matrix method for DR is neither precise in its formulation of the problem, nor reliably accurate in its determination of DR data, nor computationally efficient. Perturbation methods, on the other hand, do not suffer from any of these shortcomings, and are ideally suited for determining RR+DR rate coefficients for the modeling of x ray photoionized plasmas.

## ACKNOWLEDGMENTS

T.W.G. was supported in part by NASA Space Astrophysics Research and Analysis Program Grant No. NAG5-10448. NRB was supported by UK PPARC Grant No. PPA/G/S/1997/00783. DWS was supported in part by NASA Space Astrophysics Research and Analysis Program Grant No. NAG5-5261.

- 
- [1] F. Paerels, J. Cottam, M. Sako, D.A. Liedahl, A.C. Brinkman, R.L.J. van der Meer, J.S. Kaastra, and P. Predehl, *Astrophys. J.* **533**, L135 (2000).
- [2] S. Kaspi, W.N. Brandt, R. Sambruna, G. Chartas, G.P. Garmire, and J.A. Nousek, *Astrophys. J.* **535**, L17 (2000).
- [3] M. Sako, S.M. Kahn, F. Paerels, and D.A. Liedahl, *Astrophys. J.*, **543**, L115 (2000).
- [4] M. Sako *et al.*, *Astron. Astrophys.* **365**, L168 (2001).
- [5] J. Cottam, S.M. Kahn, A.C. Brinkman, J.W. den Herder, and C. Erd, *Astron. Astrophys.* **365**, L277 (2001).
- [6] D.W. Savin, S.M. Kahn, J. Linkeman, A.A. Saghir, M. Schmitt, M. Grilser, R. Repnow, D. Schwalm, A. Wolf, T. Bartsch, C. Brandau, A. Hoffknecht, A. Müller, S. Schippers, M.H. Chen, and N.R. Badnell, *Astrophys. J., Suppl. Ser.* **123**, 687 (1999).
- [7] D.W. Savin, N.R. Badnell, T. Bartsch, E. Behar, C. Brandau, M.H. Chen, M. Grieser, T.W. Gorczyca, G. Gwinner, A. Hoffknecht, S.M. Kahn, A. Müller, R. Repnow, A.A. Saghir, S. Schippers, M. Schmitt, D. Schwalm, A. Wolf, and P.A. Závodszky, in *Proceedings of the 12th APS Topical Conference on Atomic Processes in Plasmas, Reno, Nevada*, edited by R. C. Mancini and R. A. Phaneuf AIP Conf. Proc. No. **547** (AIP, Melville, New York, 2000), p.267.
- [8] T.R. Kallman and M. Bautista, *Astrophys. J., Suppl. Ser.* **133**, 321 (2001).
- [9] D.W. Savin, T. Bartsch, M.H. Chen, S.M. Kahn, D.A. Liedahl, J. Linkemann, A. Müller, S. Schippers, M. Schmitt, D. Schwalm, and A. Wolf, *Astrophys. J.* **489**, L115 (1997).
- [10] D. W. Savin, E. Behar, S. M. Kahn, G. Gwinner, A. A. Saghir, M. Schmitt, M. Grieser, R. Repnow, D. Schwalm, A. Wolf, T. Bartsch, A. Müller, S. Schippers, N. R. Badnell, M. H. Chen, and T. W. Gorczyca, *Astrophys. J., Suppl. Ser.* **138**, 337 (2002).
- [11] N.R. Badnell, *J. Phys. B* **19**, 3827 (1986).
- [12] M.H. Chen, *Phys. Rev. A* **31**, 1449 (1985).
- [13] A. Bar-Shalom, M. Klapisch, and J. Oreg, *J. Quant. Spectrosc. Radiat. Transf.* **71**, 168 (2001).
- [14] F. Robicheaux, T.W. Gorczyca, M.S. Pindzola, and N.R. Badnell, *Phys. Rev. A* **52**, 1319 (1995).



- [15] A.K. Pradhan, S.N. Nahar, and H.L. Zhang, *Astrophys. J.* **549**, L268 (2001).
- [16] H.L. Zhang, S.N. Nahar, and A.K. Pradhan, *Phys. Rev. A* **64**, 032719 (2001).
- [17] P. G. Burke and K. A. Berrington, *Atomic and Molecular Processes: An R-matrix Approach* (IOP Publishing, Bristol, 1993).
- [18] [http://amdpp.phys.strath.ac.uk/UK\\_RmaX](http://amdpp.phys.strath.ac.uk/UK_RmaX)
- [19] K.A. Berrington, W.B. Eissner, and P.H. Norrington, *Comput. Phys. Commun.* **92**, 290 (1995).
- [20] N.S. Scott and K.T. Taylor, *Comput. Phys. Commun.* **25**, 347 (1982).
- [21] A.P. Hickman, *J. Phys. B* **17**, L101 (1984).
- [22] F. Robicheaux, *J. Phys. B* **31**, L109 (1998).
- [23] R.H. Bell and M.J. Seaton, *J. Phys. B* **18**, 1589 (1985).
- [24] T.W. Gorczyca, F. Robicheaux, M.S. Pindzola, and N.R. Badnell, *Phys. Rev. A* **52**, 3852 (1995).
- [25] T.W. Gorczyca, F. Robicheaux, M.S. Pindzola, and N.R. Badnell, *Phys. Rev. A* **54**, 2107 (1996).
- [26] C. Froese Fischer, *Comput. Phys. Commun.* **64**, 369 (1991).
- [27] M.J. Seaton, *Rep. Prog. Phys.* **46**, 167 (1983).
- [28] M. Aymar, C.H. Greene, and E. Luc-Koenig, *Rev. Mod. Phys.* **68**, 1015 (1996).
- [29] T.W. Gorczyca and N.R. Badnell, *J. Phys. B* **29**, L283 (1996).
- [30] N.R. Badnell, T.W. Gorczyca, and A.D. Price, *J. Phys. B* **31**, L239 (1998).
- [31] F. Robicheaux, *Phys. Rev. A* **48**, 4162 (1993).
- [32] M. Arnaud and J. Raymond, *Astrophys. J.* **398**, 394 (1992).
- [33] U. Fano, *Phys. Rev. A* **2**, 353 (1970).
- [34] T.W. Gorczyca, Z. Felfli, H.-L. Zhou, and S.T. Manson, *Phys. Rev. A* **58**, 3661 (1998).
- [35] A.A. Wills, T.W. Gorczyca, N. Berrah, B. Langer, Z. Felfli, E. Kukk, J.D. Bozek, O. Nayandin, and M. Alshehri, *Phys. Rev. Lett.* **80**, 5085 (1998).
- [36] N. Haque, H.S. Chakraborty, P.C. Deshmukh, S.T. Manson, A.Z. Msezane, N.C. Deb, Z. Felfli, and T.W. Gorczyca, *Phys. Rev. A* **60**, 4577 (1999).
- [37] T.W. Gorczyca, Z. Felfli, N.C. Deb, and A.Z. Msezane, *Phys. Rev. A* **63**, 010702 (2000).
- [38] N.R. Badnell and D.C. Griffin, *J. Phys. B* **32**, 2267 (1999).
- [39] M.S. Pindzola, N.R. Badnell, and D.C. Griffin, *Phys. Rev. A* **46**, 5725 (1992).
- [40] T.W. Gorczyca and N.R. Badnell, *Phys. Rev. Lett.* **79**, 2783 (1997).